Biological Psychiatry: GOS

Archival Report

A cAMP-Related Gene Network in Microglia Is Inversely Regulated by Morphine Tolerance and Withdrawal

Kevin R. Coffey, Atom J. Lesiak, Ruby E. Marx, Emily K. Vo, Gwenn A. Garden, and John F. Neumaier

ABSTRACT

BACKGROUND: Microglia have recently been implicated in opioid dependence and withdrawal. Mu opioid receptors are expressed in microglia, and microglia form intimate connections with nearby neurons. Accordingly, opioids have both direct (mu opioid receptor mediated) and indirect (neuron interaction mediated) effects on microglia function.

METHODS: To investigate this directly, we used RNA sequencing of ribosome-associated RNAs from striatal microglia (RiboTag sequencing) after the induction of morphine tolerance and followed by naloxone-precipitated withdrawal (n = 16). We validated the RNA sequencing data by combining fluorescent in situ hybridization with immunohistochemistry for microglia (n = 18). Finally, we expressed and activated the $G_{i/o}$-coupled hM_4Di DREADD (designer receptor exclusively activated by designer drugs) in *Cx3cr1*-expressing cells during morphine withdrawal (n = 18).

RESULTS: We detected large, inverse changes in RNA translation following opioid tolerance and withdrawal. Weighted gene coexpression network analysis revealed an intriguing network of cyclic adenosine monophosphate (cAMP)-associated genes that are known to be involved in microglial motility, morphology, and interactions with neurons that were downregulated with morphine tolerance and upregulated rapidly by withdrawal. Three-dimensional histological reconstruction of microglia allowed for volumetric, visual colocalization of messenger RNA within individual microglia that validated our bioinformatics results. Direct activation of hM_4Di in *Cx3cr1*-expressing cells exacerbated signs of opioid withdrawal rather than mimicking the effects of morphine.

CONCLUSIONS: These results indicate that G_i signaling and cAMP-associated gene networks are inversely engaged during opioid tolerance and early withdrawal, perhaps revealing a role of microglia in mitigating the consequences of opioids.

https://doi.org/10.1016/j.bpsgos.2021.07.011

Opioid abuse has reached epidemic proportions in the United States and is responsible for more than 40,000 overdose deaths each year (1,2). While the motivations for drug use are complex, the threat of withdrawal provokes anticipatory anxiety and avoidance of treatment seeking. Besides substitution therapy, current treatments for opioid withdrawal are not sufficiently effective, and developing new strategies for diminishing withdrawal may improve adherence to opioid abstinence. There are consistent mu opioid receptor (MOR)–dependent gene networks that are regulated in the opioid abstinent brain (3–5) and are the target of therapeutic manipulation in neurons (6). However, there is accumulating evidence that other cell types, including microglia, play a prominent role in drug addiction and withdrawal (7–10).

The interface of opioids, microglia, and neuroinflammation is an emerging field, but there is now a substantial body of evidence that MORs are expressed in microglia (11–14), including in the present dataset, where we found consistent MOR (*Oprm1*) translation in striatal microglia. Microglia also form intimate connections with neurons and sense neuronal excitability (15,16), so opioids likely have both direct (MOR mediated) and indirect (neuron-microglia interaction mediated) effects on microglia function. Opioid administration decreases the density of IBA1-positive microglia in cortex and striatum, which is increased again after spontaneous withdrawal (17). Microglia inhibition by minocycline or ibudilast (18) or blocking microglia pannexin channels (19) produces a dose-dependent reduction in opioid withdrawal behaviors. Opioid withdrawal can intensify pain sensitivity that appears to involve proinflammatory processes, including activation of toll-like receptors TLR2 and TLR4, the NLRP3 inflammasome, and nuclear factor-κB (20–24), suggesting that withdrawal engages delayed microglial activation. Opioids are used cyclically, so that repeated exposures/withdrawals may prime or condition microglia (17) to produce an exaggerated immune response to subsequent cycles. While several studies of microglia have examined later stages in this process, we hypothesized that microglia function and gene expression are altered rapidly,

Published by Elsevier Inc on behalf of Society of Biological Psychiatry. This is an open access article under the CC BY-NC-ND license (http://creativecommons.org/licenses/by-nc-nd/4.0/).

ISSN: 2667-1743

even during the immediate behavioral changes associated with precipitated withdrawal.

One method for assessing rapidly evolving adaptations to environmental challenges is to investigate RNA translation. Microglial ribosomes are expressed in fine processes where they are presumed to translate messenger RNA (mRNA) locally, similar to astrocytes (25). Fine processes are not recovered by mechanical methods of isolating microglia, and fluorescence-activated cell sorting of microglia significantly alters immediate early gene expression compared with RNA isolation using ribosome pulldown (26). Thus, we decided to use the RiboTag strategy to immunopurify ribosome-associated mRNAs specifically from microglia. This approach provides an excellent yield of highly enriched microglia mRNA molecules actively undergoing translation. We used a well-characterized morphine administration schedule that produces tolerance (4) and collected ribosome-associated mRNA to provide the first complete picture of the translational consequences of opioid tolerance and withdrawal on striatal microglia. Using weighted gene coexpression network analysis (WGCNA), we identified a network of mRNA actively undergoing translation in microglia that are markedly inhibited by opioid tolerance and rapidly reversed by naloxone-precipitated withdrawal. This expression pattern was validated among key genes in the network through three-dimensional colocalization of IBA1 immunohistochemistry (IHC) signal and fluorescent in situ hybridization (FISH) signal. Intriguingly, many of the mRNAs are related to cyclic adenosine monophosphate (cAMP) signaling, and inhibiting cAMP-mediated signaling using $G_{i/o}$-coupled hM_4Di DREADD (designer receptor exclusively activated by designer drugs) activation in *Cx3cr1*-expressing cells exacerbated the acute behavioral signs of withdrawal. Together, these data suggest that microglia are actively involved in both opioid tolerance and acute withdrawal through a compensatory cAMP-mediated mechanism.

METHODS AND MATERIALS

Animals

Experiments were performed in compliance with the Guide for the Care and Use of Laboratory Animals and were approved by the Institutional Animal Care and Use Committee, University of Washington.

Experimental Design

Male and female mice were generated by crossing tamoxifen-inducible *Cx3cr1*-CreERT2 hemizygous mice with homozygous floxed RiboTag mice on a C57BL/6 background (Figure 1A). Mice received tamoxifen (75 mg/kg via intraperitoneal injection [ip]) for 7 days at 6 weeks (Figure 1B). A 2 × 2 treatment design (n = 6/group) yielded 4 groups: saline+saline (SS), saline+naloxone (SN), morphine+saline (MS), and morphine+naloxone (MN) (Figure 1B). At approximately 11 weeks, mice received either morphine or saline twice daily for 5 days. Morphine dose escalated daily: 20 mg/kg ip (day 1), 40 mg/kg ip (day 2), 60 mg/kg ip (day 3), 80 mg/kg ip (day 4), 100 mg/kg ip (day 5). On day 6, mice received 100 mg/kg ip morphine or saline. Two hours later, they received either naloxone (1 mg/kg via subcutaneous injection) or saline and were video recorded for 30 minutes in individual cages from above. Videos were automatically analyzed for withdrawal metrics (distance, contraction, and immobility) using EthoVision XT 11 (Noldus) and custom MATLAB scripts (The Mathworks, Inc.). Contraction was defined as <65% maximum body length (hunching), and immobility was defined as <2 cm/s of movement. Mice were sacrificed 2 hours after naloxone/vehicle injection, and brains were rapidly extracted for RNA processing (Figure 1D).

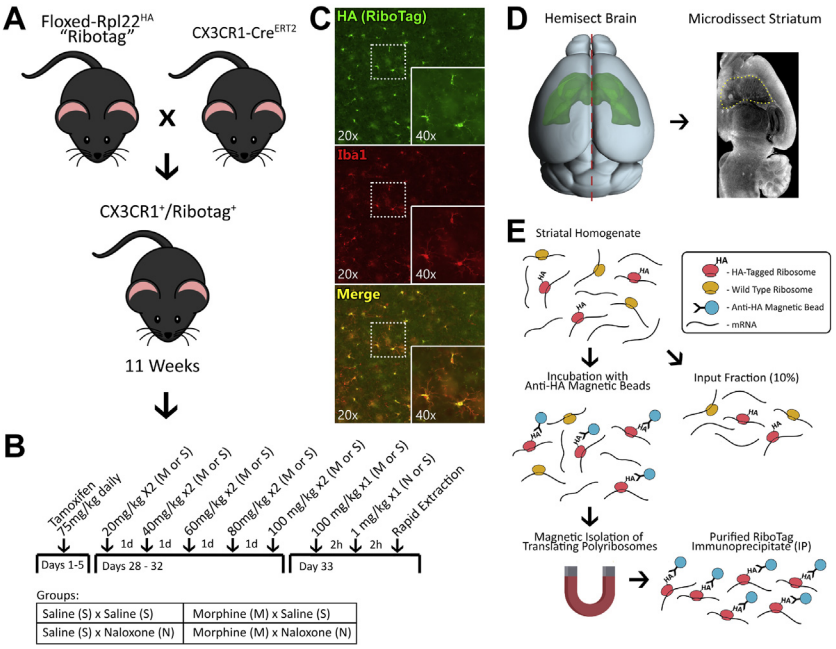

Figure 1. Experimental overview. **(A)** Experimental male and female mice were generated by crossing tamoxifen-inducible *Cx3cr1*-CreERT2 hemizygous mice with homozygous floxed RiboTag mice. **(B)** The experiment was performed as a 2 × 2 design (n = 6/group) with all mice receiving tamoxifen for 5 days at 6 weeks of age. At approximately 11 weeks of age, the mice received either morphine or saline for 5 days on an escalating twice-daily schedule. On day 6, the mice received 100 mg/kg morphine via intraperitoneal injection or equivalent volume saline. Two hours later, they received either naloxone (1 mg/kg subcutaneous) or saline. **(C)** In experimental animals, RiboTag immunostaining colocalized exclusively with IBA1 immunostaining. **(D)** Brains were rapidly extracted and hemisected, and the striatum was microdissected and homogenized for RiboTag. **(E)** RiboTag isolation was accomplished by incubating homogenized tissue with anti-HA magnetic beads and performing magnetic isolation of ribosome bound RNAs. HA, hemagglutinin.

Four samples from each group (2 males, 2 females; total n = 16) were processed for sequencing. While we included males and females, the RNA sequencing (RNA-Seq) analysis was not powered to examine for differences in microglial gene expression between sexes. Throughout the article, MS animals are compared with SS animals when discussing the effects of tolerance, while MN animals are compared with MS animals when discussing withdrawal. Twice-daily morphine schedules, both single and escalating dose, have been shown to rapidly induce analgesic tolerance and increase locomotor sensitization (27,28). However, in the present article, tolerance refers more generally to the animal's ability to endure high doses of morphine (100 mg/kg) without severe consequences.

RiboTag-Seq Processing

Briefly, striatal dissections were homogenized in supplemented homogenization buffer, samples were centrifuged, and supernatant was collected. From each sample, 10% was set aside as the whole transcriptome sample (input), and the remaining sample was processed to isolate ribosome bound mRNA (immunoprecipitate [IP]) (Figure 1E). All aspects of tissue processing, immunoprecipitation, and RNA-Seq libraries generation are described in detail in our previous RiboTag-Seq article (29). In the present study, control mice with no tamoxifen were used to generate the negative control samples. Raw FastQ files were processed through the Galaxy platform (30). FastQ files were inspected for quality using FastQC (Galaxy Version 0.7.0) and then passed to Salmon (Galaxy Version 0.8.2) (31) for quantification of transcripts. The Salmon index was built using the protein coding transcriptome GRCm38/mm10. A small fraction of mRNA captured during immunoprecipitation is nonspecific. To mitigate this, we used a computational approach to remove input contamination from IP samples (32). All IP data presented in the main article has undergone this adjustment (Supplemental Methods).

Differential Expression Analysis

Differential gene expression was calculated using DESeq2 (Galaxy Version 2.11.39; default settings) (33). To determine microglia-specific gene enrichment, all IP samples were compared with all input samples. To determine the effects of naloxone alone, SN IP samples were compared with SS IP samples. For morphine tolerance, MS IP samples were compared with SS IP samples. For withdrawal, MN IP samples were compared with MS IP samples. A positive Wald statistic means a gene was expressed more in the first group (false discovery rate; q = .10).

Gene Set Enrichment Analysis

Wald statics generated by DeSeq2 were used as the ranking variable for gene set enrichment analysis (GSEA). All genes with reliable statistical comparisons (those not filtered by DeSeq2) were entered into WebGestalt 2019 (34), and GSEA was run on all pertinent comparisons. Gene sets analyzed include GO: Biological Process, GO: Molecular Function, KEGG, Wiki Pathway, Transcription Factor Targets, and MicroRNA Targets.

Weighted Gene Coexpression Network Analysis

WGCNA and module clustering were accomplished using the WGCNA (35) package for R (36). Briefly, the gene count matrix for all IP samples was filtered to remove zero-variance genes, and a signed topological overlap matrix was generated for clustering. Module membership was assigned using a dynamic tree cut, and highly correlated modules were merged by reclustering module eigengenes. Gene modules were randomly renamed using the Crayola Color Palette to combat attribution of meaning or importance to numbered modules (37).

Post-processing of the topological overlap matrix was completed with a custom MATLAB class (@WGCNA). This class allows for simple object-based analysis of complex WGCNA data. Topological overlap matrices, module membership files, and DeSeq files can be loaded into a single "W" object. @WGCNA allows for calculation and visualization of module eigengenes, merging of modules, analyses of module membership, and differential expression. @WGCNA uses the powerful graphing and network analysis functions of MATLAB to generate complete-genome network graphs with module membership or differential expression markers, two-dimensional or three-dimensional graphs from individual modules or individual genes, and includes settings for edge pruning, node appearance, and edge appearance. @WGCNA is available at GitHub.com/MxMarx/WGCNA.

FISH Validation of Changes in Key cAMP-Related mRNA

A new cohort of mice (n = 18, 6/group, 3 males and 3 females) was subjected to our morphine tolerance and withdrawal procedure (no SN group). Tissue was dual processed for fluorescent in situ hybridization (FISH) and IBA1 IHC. Two hours following naloxone administration, mice were anesthetized and perfused with phosphate-buffered saline (PBS), followed by 4% paraformaldehyde. Brains were post-fixed in 4% paraformaldehyde for 48 hours then transferred to 30% sucrose in PBS. Sections (14 μm) were mounted 6 brains/slide covering all conditions (1 male, 1 female × SS, MS, MN). RNAscope (Advanced Cell Diagnostics, Inc.) was used to visualize target mRNA; protease incubation was limited to 10 minutes. IBA1 IHC was performed following RNAscope. Tissue was blocked with 4% bovine serum albumin (Thermo Fisher Scientific) and 0.3% Triton (Sigma-Aldrich) in PBS for 1 hour at room temperature, incubated with anti-IBA1 rabbit antibody (1:500; Fujifilm Cellular Dynamics) in blocking solution for 18 hours at 4 °C, rinsed (PBS; 3× 10 min), incubated with Alexa-Fluor 488 Goat anti-Rabbit in blocking solution (1:400; Thermo Fisher Scientific) for 60 minutes at room temperature, rinsed (PBS; 3× 10 min), and cover slipped with ProLong Gold Antifade Mountant with DAPI (Thermo Fisher Scientific). Confocal stacks (10 μm at 40× with 1.25× zoom) of the striatum (anterior-posterior 0 mm, medial-lateral 2 mm, dorsal-ventral −3 mm) were acquired on a Leica SP8 X confocal microscope (Leica Microsystems). Individual microglia reconstruction and colocalization analysis was performed using custom MATLAB scripts. Images were processed in a blind batch, and all settings remained identical.

IHC and Image Analysis for Microglia Morphology

A new cohort of mice (n = 12, 4/group, 2 males and 2 females) was subjected to the above morphine tolerance and withdrawal procedure (no SN group). Two hours following naloxone injections, brains were removed and post-fixed as described above. Sections (40 μm) of the striatum were collected on a sliding freezing microtome. Free-floating sections were processed for IBA1 IHC as described above. Confocal stacks (30 μm at 40× with 1× zoom) of the striatum (anterior-posterior 0 mm, medial-lateral 2 mm, dorsal ventral −3 mm) were acquired on a Leica SP8 X confocal microscope. Images from this cohort and from the RNAscope experiment were analyzed together for morphological analysis. Individual microglia reconstruction and quantification was performed using 3DMorph software (38). Images were processed in a blind batch, and all image analysis settings remained identical. Morphological parameters (volume, branch points, end points) were calculated and normalized to stack depth and image resolution.

Chemogenetic Inhibition of cAMP Signaling in *Cx3cr1*-Expressing Cells via hM_4Di

Experimental animals were generated by crossing mice that are hemizygous for tamoxifen-inducible *Cx3cr1*-Cre^{ERT2} with mice that are hemizygous for floxed hM_4Di. Tamoxifen induction of Cre was performed as described above. Two groups of *Cx3cr1*-hM_4Di and 1 group of *Cx3cr1*-Cre^{ERT2} control animals with 3 males and 3 females per group were used (total n = 18). All animals received escalating morphine as described in above; 2 hours after the final morphine injection (100 mg/kg ip), the mice received either clozapine N-oxide (CNO) (3 mg/kg ip) or 2% dimethylsulfoxide vehicle 20 minutes before naloxone (1 mg/kg subcutaneous). Withdrawal was automatically scored using the same custom MATLAB script described above.

Statistical Analyses

For analyses not involving bioinformatics, analysis of variance was followed by Dunn-Sidak–corrected contrasts.

Code and Data Availability

All RNA-Seq files and the RNA-Seq pipeline are available on our Galaxy Server. All code and data used for the figures are available in the supplementary code and data.

RESULTS

Morphine Tolerance Causes Locomotor Sensitization While Naloxone Precipitates Withdrawal

Mice were administered drug (morphine or saline) for 6 days, then given a treatment (naloxone or saline). There was a significant main effect of drug on distance traveled ($F_{1,15}$ = 10.8, p = .005) and a significant interaction of drug × treatment ($F_{1,15}$ = 23.4, p < .01). Morphine tolerant mice displayed robust locomotor sensitization, traveling a significantly greater distance than any other group (Figure S1B; *p < .01). There was also a significant main effect of drug on hunched body contraction ($F_{1,15}$ = 6.6, p = .021) and a significant interaction of drug × treatment ($F_{1,15}$ = 6.2, p = .025). Mice in withdrawal spent more time hunched than any other group (Figure S1C; *p < .01). There was also a significant interaction of drug × treatment on immobility ($F_{1,15}$ = 26.3, p < .01). Mice in withdrawal stayed immobile longer than any other group (Figure S1D; *p < .01). Morphine-naïve mice treated with naloxone did not differ from morphine-naïve mice treated with saline.

Immunoprecipitation and Sequencing

Ribotag IHC signal colocalized with IBA1 IHC signal, including in microglia processes (Figure 1C). RNA extraction from input samples yielded 120 ± 11 ng (mean ± SEM) of RNA, while IP samples yielded 51 ± 4 ng (mean ± SEM) of RNA. RNA-Seq from input samples yielded 4.1 ± 0.5 million reads (mean ± SEM), while IP samples yielded 2.8 ± 0.2 million reads (mean ± SEM).

Microglia-Specific Markers Are Enriched in RiboTag-Seq Samples

Differential expression analysis of IP versus input samples showed dramatic enrichment of microglia-specific RNAs (Figure 2A). Among the most enriched genes were canonical microglia markers, such as *C1qa*, *Tmem119*, and *Itgam* (CD11b) (Figure 2A). Common microglia signaling pathways, such as cytokine binding, purinergic receptor activity, and nuclear factor-κB binding, were enriched in IP samples (Figure 2B). Normalized counts from IP samples were compared with the top 1000 genes from available single-cell RNA-Seq data for 6 presumed cell types (39). Presumed microglia markers were detected at high levels in our IP data, while markers for other cell types were detected at low levels (Figure 2C). Using t-distributed stochastic neighbor embedding, IP samples were shown to be markedly different from input samples (Figure 2D).

Morphine Tolerance and Withdrawal Produce Inverse Patterns of Differential Gene Expression

Naloxone administration to morphine-naïve animals yielded very few differentially expressed genes in microglia (SN vs. SS) (Figure 3A). Morphine tolerance produced robust changes in microglia, with a similar number of upregulated and downregulated genes (555 up and 653 down; MS vs. SS) (Figure 3B). By contrast, withdrawal produced a dramatic upregulation in genes with roughly half as many downregulated (706 up and 344 down; MN vs. MS) (Figure 3C). For differentially expressed genes, there was a significant inverse relationship between expression changes during morphine tolerance and withdrawal (R^2 = 0.86, p < .01) (Figure 3D). Genes that were downregulated during morphine tolerance were upregulated during withdrawal and vice versa. Using t-distributed stochastic neighbor embedding, tolerant and withdrawn animals were shown to be markedly different from saline animals (Figure 3E). Input sample analyses are available in the supplementary code and data.

Morphine Tolerance and Withdrawal Produce Inverse Regulation of Annotated Gene Sets

GSEA is a method of inferring biological meaning from differential expression data based on previously annotated data

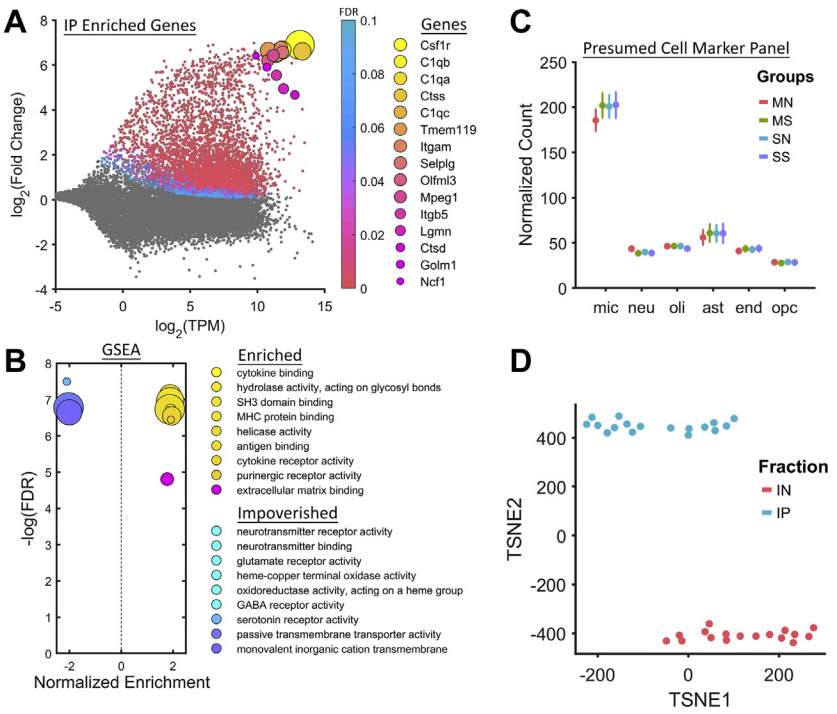

Figure 2. RiboTag enriches microglia markers. **(A)** RiboTag sequencing samples are dramatically enriched with microglia markers such as *Tmem119* and *Itgam* (CD11b). **(B)** GSEA reveals an upregulation of genes associated with canonical microglia gene sets, such as cytokine binding and purinergic receptor activity. **(C)** Presumed cell markers for microglia are highly enriched in the IP samples compared with markers for neurons, oligodendrocytes, astrocytes, endothelial cells, and oligodendrocyte progenitor cells. **(D)** IP samples are easily separated from IN samples using TSNE. ast, astrocytes; end, endothelial cells; FDR, false discovery rate; GABA, gamma-aminobutyric acid; GSEA, gene set enrichment analysis; IN, input; IP, immunoprecipitate; MHC, major histocompatibility complex; mic, microglia; MN, morphine+naloxone; MS, morphine+saline; neu, neurons; oli, oligodendrocytes; opc, oligodendrocyte progenitor cells; SN, saline+naloxone; SS, saline+saline; TSNE, t-distributed stochastic neighbor embedding.

sets. In brief, this analysis revealed inverse changes in numerous annotated gene sets, in particular, gene sets involved in the unfolded protein response and regulation of synaptic structure and function (Figure S2). Interactive HTML files for IP and input GSEA are available in the supplementary code and data.

Morphine Tolerance and Withdrawal Produce Inverse Regulation of a cAMP-Associated Gene Network

WGCNS (35) was used as an unbiased clustering strategy to identify sets of related genes, including those that were

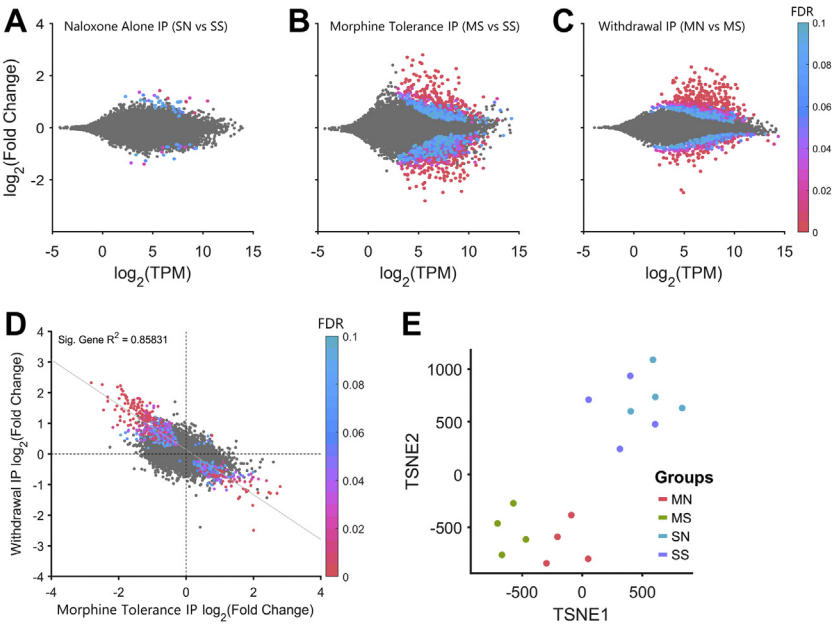

Figure 3. Morphine tolerance and withdrawal induce inverse differential expression in microglia. **(A)** Naloxone administration to morphine-naïve animals has little effect on gene expression in the IP samples. **(B)** Morphine tolerance produces roughly equal numbers of upregulated and downregulated differentially expressed genes, and **(C)** naloxone-precipitated withdrawal produces mainly upregulation of differentially expressed genes. **(D)** Differential expression during withdrawal vs. morphine tolerance is inversely correlated. **(E)** Saline, morphine, and withdrawal animals are differentiable based on TSNE. FDR, false discovery rate; IP, immunoprecipitate; MN, morphine+naloxone; MS, morphine+saline; SN, saline+naloxone; SS, saline+saline; TPM, transcript count per million; TSNE, t-distributed stochastic neighbor embedding.

differentially regulated by morphine tolerance and withdrawal (40). The resulting network analysis for the entire RiboTag-Seq dataset is shown in a minimum spanning tree (Figure 4A). Highly significant differentially expressed genes formed modules that often overlap for morphine tolerance (Figure 4B) and withdrawal (Figure 4C). Of particular interest are modules that were differentially expressed between treatment groups, such as the Sheen Green module, which was downregulated during morphine tolerance and upregulated during withdrawal (Figure S3). Individual genes and their network connections were visualized via a circle-network graph (Figure 4D), where the color of each connecting line reflects the statistical similarity between individual gene pairs. Another conventional way to represent these relationships is with hub and spoke graphs (Figure 4E); however, hub genes should not be misconstrued as directly regulating their neighbors. Rather, these most central genes best reflect the patterns of their neighbors and the module overall (Figure 4E).

WGCNA does not take into consideration the presumed function of genes, yet the Sheen Green network contains a set of genes that, on inspection, are indeed functionally related. Many of these genes are downstream targets of cAMP signaling and promote reorganization of synapses and the actin cytoskeleton (Figure 4F). Repeated morphine administration produced a negative correlation between network centrality and differential expression of individual genes in the

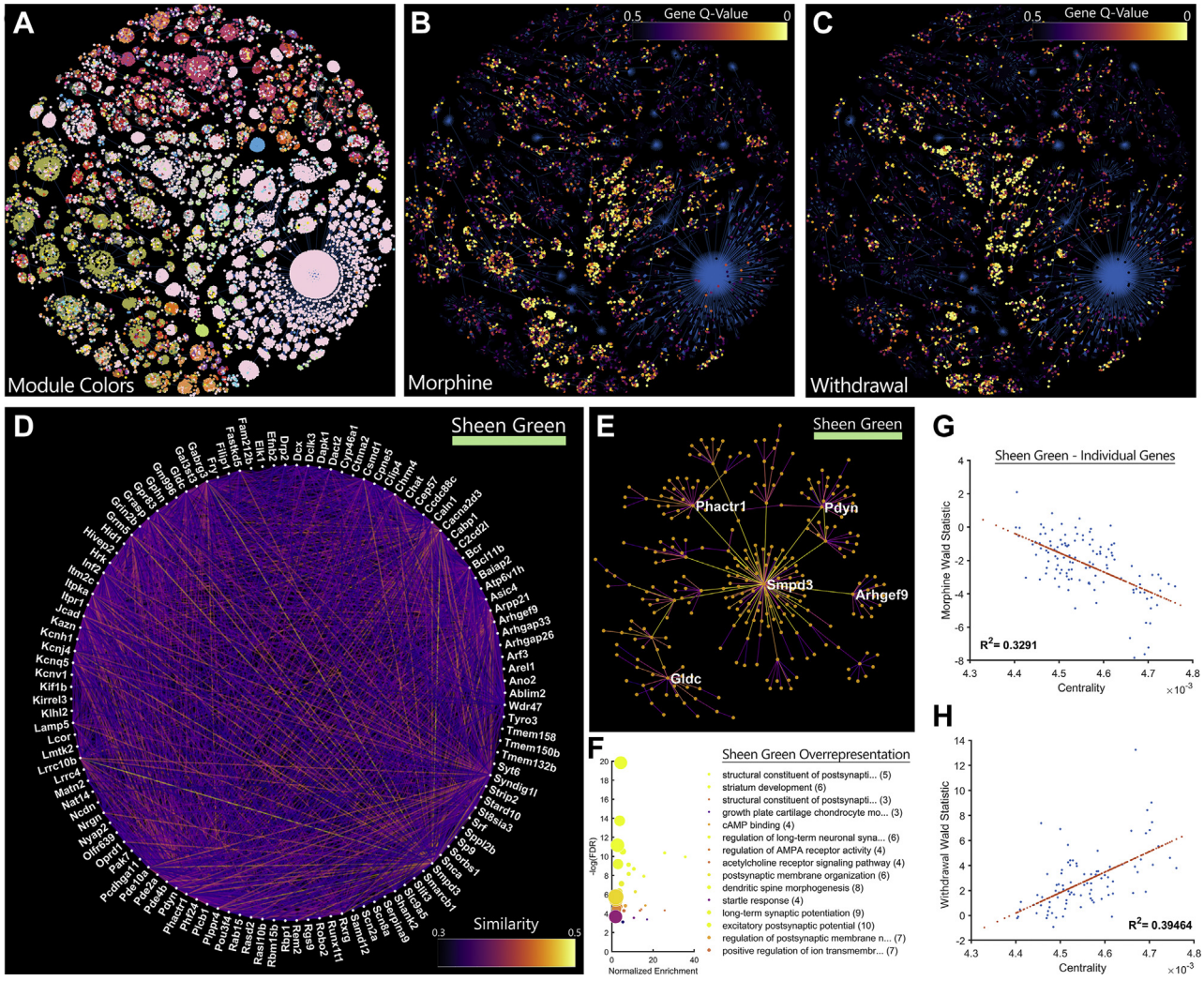

Figure 4. A cAMP-regulated gene network is inhibited by morphine tolerance and induced by withdrawal. **(A)** Genes are coded by module color and projected into a two-dimensional minimum spanning tree. The same genes are coded by differential expression (*q* value) data during **(B)** morphine tolerance and **(C)** withdrawal. Functionally related genes tend to cluster in modules. **(D)** The Sheen Green gene module is displayed using a circle layout. Line brightness represents gene similarity as calculated by weighted gene coexpression network analysis. **(E)** The top 5 most central genes in each network are highlighted in a hub-and-spoke representation of the network. **(F)** Overrepresentation analysis of genes in this network provides clues to their functional relevance. Many genes are downstream targets of cAMP signaling or promote reorganization of synapses and the actin cytoskeleton. Gene sets are sorted by normalized enrichment, while color represents −log(FDR). Centrality in the Sheen Green network is highly correlated to differential expression for both **(G)** morphine tolerance and **(H)** withdrawal. cAMP, cyclic adenosine monophosphate; FDR, false discovery rate.

Sheen Green module (MS vs SS) (Figure 4G), whereas withdrawal produced the inverse pattern (MS vs. SS) (Figure 4H). The more central a gene was to the Sheen Green module, the more strongly it was differentially regulated by opioid tolerance and withdrawal. Other modules that may be of interest, along with all data from the input samples, can be reviewed in the supplementary code and data.

Validation of Key cAMP-Related Genes That Are Inhibited by Tolerance and Induced by Withdrawal

Tissue from a new cohort of mice was dual processed for IBA1 IHC and FISH, then imaged by confocal microscopy to permit accurate three-dimensional colocalization of mRNA signals within striatal microglia. The percent of microglia expressing *Pde10a* (a cAMP hydrolyzing phosphodiesterase) was significantly different across groups ($F_{2,15} = 3.8$, $p = .047$) (Figure 5B), as was the *Pde10a* signal in microglia ($F_{2,15} = 5.0$, $p = .021$) (Figure 5C); both *Pde10a*-expressing microglia and *Pde10a* signal were reduced by morphine tolerance (Figure 5B, C; $^*p < .05$), with a trend toward reversal during withdrawal. *Arpp21* (a cAMP-regulated phosphoprotein) signal in microglia was significantly different across groups ($F_{2,15} = 3.8$, $p = .047$) (Figure 5F). Microglia *Arpp21* signal was increased by withdrawal (Figure 5F; $^*p < .05$). The percent of microglia expressing *Drd1* (a G_s-coupled, cAMP-stimulating receptor) was also significantly different across groups ($F_{2,15} = 4.5$, $p = .030$) (Figure 5H), as was *Drd1* signal in microglia ($F_{2,15} = 9.6$, $p = .002$) (Figure 5I). *Drd1* expressing microglia and *Drd1* signal

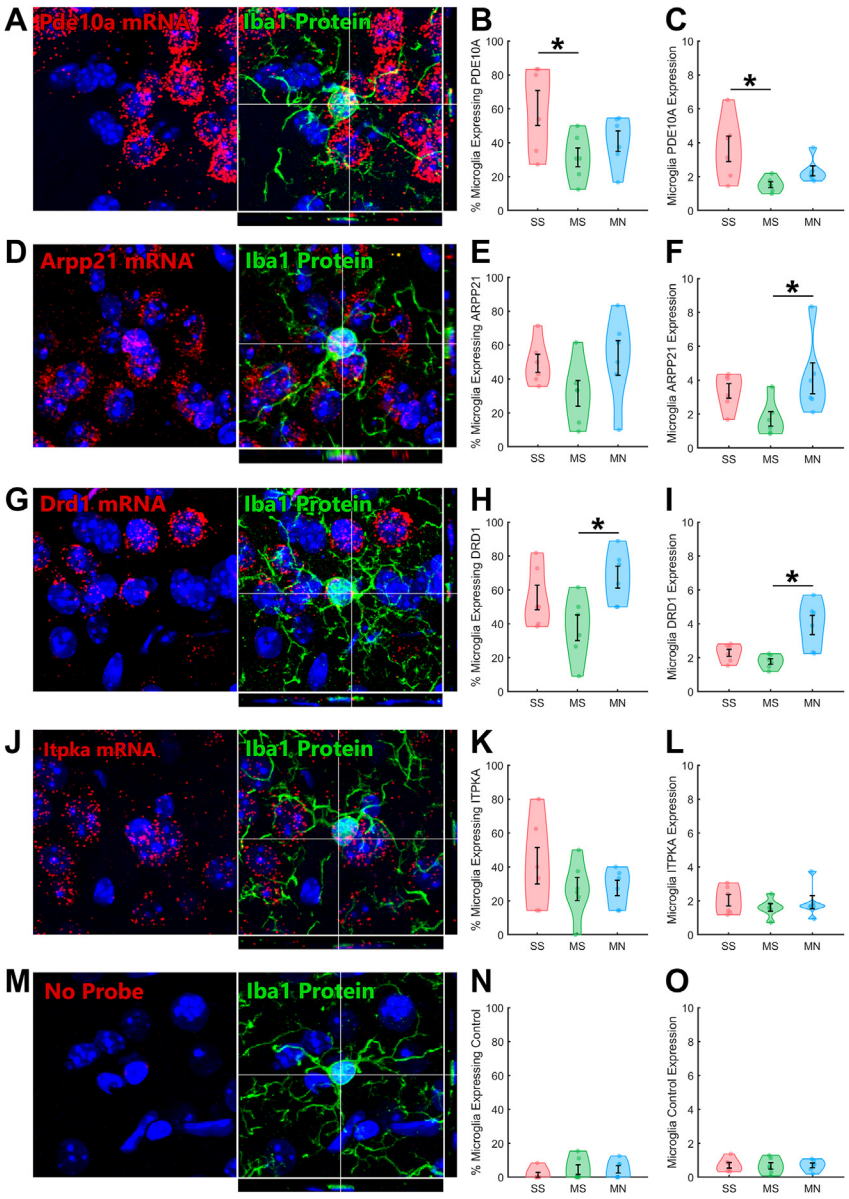

Figure 5. Key cAMP-related genes are expressed in microglia, inhibited by tolerance, and induced by withdrawal. RNAscope was combined with immunohistochemistry for IBA1 and confocal imaging to quantify three-dimensional colocalization of mRNA within microglia. **(A)** *Pde10a* is expressed in a subset of microglia. **(B)** The percent of microglia that express *Pde10a* is significantly reduced by morphine tolerance, **(C)** as is the expression of *Pde10a* in microglia. **(D)** *Arpp21* is also expressed in a subset of microglia. **(E)** The percent of microglia that express *Arpp21* appears inversely modulated by morphine and withdrawal, but groups did not significantly differ. **(F)** The expression of *Arpp21* in microglia is significantly increased by morphine withdrawal. **(G)** *Drd1* is expressed in a subset of microglia. **(H)** The percent of microglia that express *Drd1* is significantly increased by morphine withdrawal, **(I)** as is the expression of *Drd1* in microglia. **(J)** *Itpka* is expressed in a subset of microglia, but **(K, L)** is not modulated by morphine tolerance or withdrawal. **(M)** A complete set of negative control probe samples was processed with RNAscope and analyzed with the same software as the signal probes. **(N, O)** This technique has extremely low background contamination from nonspecific signal detection. *Post hoc $p < .05$. MN, morphine+naloxone; mRNA, messenger RNA; MS, morphine+saline; SS, saline+saline.

were both increased by withdrawal (Figure 5H, I; *$p < .05$). No changes were observed in *Itpka* mRNA (Figure 5J) or samples run with a negative control probe (Figure 5M).

Microglia Morphology Was Not Altered by Morphine Tolerance and Withdrawal

Confocal image stacks of microglia in the striatum from 2 cohorts of mice were analyzed using 3DMorph software (38). Despite accurate and reliable three-dimensional reconstruction of individual microglia, we found no significant differences in gross microglia morphology (cell volume, branch points, end points) (Figure S4C–H). Although we expected morphine tolerance and withdrawal to affect microglia morphology, our current imaging/analysis strategy could not resolve the fine filopodia at the tips of microglia processes that have recently been shown to respond rapidly to changes in cAMP (41). In future studies, we aim to directly study filopodia and their interactions with neurons.

Activation of hM$_4$Di in *Cx3cr1*-Expressing Cells Worsened Symptoms of Withdrawal

Given the discovery of cAMP signaling–associated gene modules, we decided to test whether manipulating cAMP signaling in *Cx3cr1*-expressing cells altered withdrawal-associated behaviors. Surprisingly, CNO pretreatment of mice expressing inhibitory hM$_4$Di DREADDs selectively in *Cx3cr1*-expressing cells exacerbated naloxone-precipitated withdrawal. The time mice spent in a hunched posture was significantly different across groups ($F_{2,15} = 5.5$, $p = .016$) (Figure 6B); CNO pretreatment increased the time mice in withdrawal spent hunched (Figure 6B; *$p < .05$). The time mice spent immobile was also significantly different across groups ($F_{2,15} = 5.1$, $p = .019$) (Figure 6B); CNO pretreatment increased the time mice in withdrawal spent immobile (Figure 6C; *$p < .05$). Directly increasing $G_{i/o}$ signaling in *Cx3cr1*-expressing cells did not mimic MOR activation, but instead aggravated the signs of withdrawal, suggesting that cAMP signaling in microglia may be important in mitigating withdrawal.

DISCUSSION

In this report, we identified dynamic changes in microglia in the absence of signals typically associated with neuroinflammation. Morphine and acute withdrawal produced inverse changes in the microglia translatome that appear to be cAMP mediated and could be related to microglia-neuron interaction. The induction of cAMP signaling in microglia may be a rapid and early compensatory response to opioid withdrawal.

Morphine Tolerance and Withdrawal Produce Inverse Impacts on the Microglial Translatome

Differential expression analysis revealed a significant inverse correlation between morphine- and withdrawal-induced changes in the microglial translatome. There was a striking overlap between these genes and previously published, abstinence-induced, MOR-dependent gene networks (4). Genes such as *Arpp21*, *Pde10a*, *Hpca*, *Drd1*, *Adora2a*, *Pdyn,* and numerous others form a transcriptional gene network that is regulated after protracted abstinence from morphine, and here we show that these same genes are rapidly regulated in the microglia translatome during naloxone-precipitated withdrawal. These genes play a central role in the WGCNA-defined gene network described in detail in this report. While many of these genes are known to be MOR and delta opioid receptor regulated, the broad range of the changes we report here suggests indirect impacts of opioid withdrawal as well.

A cAMP Responsive Gene Network in Microglia Is Inhibited by Morphine Tolerance and Induced by Withdrawal

WGCNA revealed a gene network that was inversely regulated by morphine tolerance and withdrawal. These networks include numerous downstream targets of cAMP signaling, cytoarchitectural adaptation, and modifiers of synaptic organization (Table S1). There was a strong association between an individual gene's network centrality and regulation by morphine tolerance and withdrawal. Many of these genes had not previously been associated with opioid tolerance or withdrawal in microglia, so we validated a subset of genes using RNAscope. mRNAs for *Pde10a* (a cAMP-hydrolyzing enzyme), *Arpp21* (a cAMP-regulated phosphoprotein), and *Drd1* (a cAMP-stimulating dopamine receptor) all colocalize within microglia and were inversely regulated by morphine tolerance and withdrawal. Other genes in this network suggest that microglia interact with nearby neurons during withdrawal, including *Syndig1*, which is involved in synapse organization (42), and *Phactr1*, which regulates synaptic activity, dendritic morphology, and cAMP-induced actin remodeling (43). As opioid tolerance and withdrawal induce

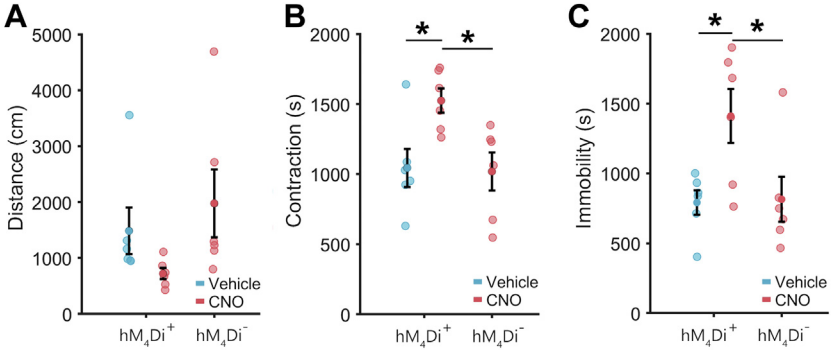

Figure 6. Activation of hM$_4$Di in microglia exacerbates withdrawal signs. **(A)** Pretreatment of *Cx3cr1*-hM$_4$Di animals with CNO produced a nonsignificant trend toward reduced locomotion during withdrawal. **(B)** Pretreatment of *Cx3cr1*-hM$_4$Di animals with CNO significantly increases body contraction during withdrawal. **(C)** Pretreatment of *Cx3cr1*-hM$_4$Di animals with CNO significantly increases immobility during withdrawal. *Cx3cr1*-hM$_4$Di animals that received vehicle and *Cx3cr1*-Cre^{ERT2} control animals that received CNO did not differ significantly on any measure. *Post hoc $p < .05$. CNO, clozapine N-oxide.

differential effects on synaptic activity (44), it is noteworthy that this microglia gene module was inversely regulated during opioid tolerance and withdrawal.

Previous literature has reported that cAMP signaling is upregulated in neurons and represents a common mechanism of reward tolerance, dependence, and withdrawal (45). A concerted upregulation of the cAMP pathway is thought to be a homeostatic adaptation to chronic opioid exposure, which serves to oppose opioid action (tolerance) and drive physical withdrawal symptoms on removal of the opioid. However, we observed a different result in microglia, where a cAMP related gene network was inversely regulated by morphine tolerance and withdrawal—apparently in the opposite direction than for neurons during opioid tolerance. While these previous studies focused on the neuronal transcriptome, the RNAs discussed here are presumed to be actively undergoing translation and may be affected by regulatory mechanisms other than transcription alone, thereby allowing for rapid and dramatic responses to conditions in the tissue. Further, the relationship between this gene network and the underlying cAMP activity is not entirely clear, as the network contains both cAMP-regulated genes and genes that regulate cAMP production and clearance. Future studies will be necessary to determine if microglia and neurons respond to opiate tolerance and withdrawal with truly inverse underlying cAMP signaling.

Microglia are thought to detect and compensate for changes in neuronal excitability in a G_i-dependent manner (32). Several receptors on microglia respond to neuronal activity, such as CX3CR1 (the fractalkine receptor) and P2Y12 (extracellular adenosine triphosphate/adenosine diphosphate receptor). Genetic deletion or inhibition of pannexin-1 (adenosine triphosphate channel) from microglia reduces the signs of opioid withdrawal (19), while P2Y12 receptors on microglia play a central role in opioid-associated hyperalgesia and neuropathic pain (46–48). Interestingly, both CX3CR1 and P2Y12 are $G_{i/o}$-coupled receptors that inhibit cAMP accumulation; it is likely that altered cAMP signaling in microglia is an important consequence of opioid withdrawal that is not directly mediated by opioid receptors.

cAMP Signaling in Striatal Microglia May Mitigate Opioid Withdrawal

The induction of cAMP-regulated genes in response to naloxone inhibition of MORs seemed counterintuitive to us, as naloxone decreases $G_{i/o}$ signaling in cells that express MORs and delta opioid receptors (including microglia). To test this notion directly, we expressed the hM_4Di DREADD selectively in *Cx3cr1*-expressing cells. The hM_4Di DREADD activates $G_{i/o}$-coupled signaling, including inhibition of adenylyl cyclase, and has been used in microglia previously (22). We found that pretreatment of these mice with CNO exacerbated the signs of opioid withdrawal. These results suggest that cAMP signaling in microglia may mitigate the acute behavioral effects of opioid withdrawal and that the increased translation of cAMP-associated genes may produce compensatory effects in microglia that protect against opioid withdrawal. A potential caveat of this interpretation is that *Cx3cr1* is expressed in cells outside the central nervous system, such as monocytes and macrophages. Because CNO was administered systemically, hM_4Di receptors on these cells may be contributing to the observed behavioral effects. In future studies, we aim to measure and manipulate microglial cAMP dynamics with greater specificity.

In summary, we used a new bioinformatics pipeline that revealed a dramatic, inverse pattern of RNA translation in striatal microglia during morphine tolerance and the early stage of opioid withdrawal. These changes in the microglia translatome were validated using FISH, appear to be cAMP mediated, and could be related to microglia-neuron interactions. Further, the induction of cAMP signaling in microglia may be an important and early compensatory response to opioid withdrawal, perhaps indicating that microglia help to mitigate withdrawal-induced neuronal hyperexcitability. Future studies should investigate microglia-specific mediators of these signaling events and explore the physical and chemical interaction between microglia and neurons that occurs during withdrawal.

ACKNOWLEDGMENTS AND DISCLOSURES

This work was supported by the National Institute on Drug Abuse (Grant Nos. R01 DA052618 [to JFN], R21 DA044757 [to JFN], K99DA052571 [to KRC], and T32 DA007278 [to KRC]).

KRC performed the experiment, analyzed the data, and wrote the manuscript. AJL performed the experiment and analyzed the data. REM analyzed the data. EKV performed the experiment. GAG provided animals, assisted in data interpretation, and wrote the manuscript. JFN designed the experiment and wrote the manuscript.

A previous version of this article was published as a preprint on bioRxiv: https://doi.org/10.1101/2020.02.10.942953

The authors report no biomedical financial interests or potential conflicts of interest.

ARTICLE INFORMATION

From the Puget Sound VA Health Care System (KRC, REM, EKV, JFN); Departments of Psychiatry & Behavioral Sciences (KRC, REM, EKV, JFN) and Genome Sciences (AJL), University of Washington School of Medicine, Seattle, Washington; and Department of Neurology (GAG), University of North Carolina, Chapel Hill, North Carolina.

Address correspondence to John F. Neumaier, M.D., Ph.D., at neumaier@uw.edu.

Received Jun 15, 2021; revised Jun 29, 2021; accepted Jul 27, 2021.

Supplementary material cited in this article is available online at https://doi.org/10.1016/j.bpsgos.2021.07.011.

REFERENCES

1. O'Donnell JK, Halpin J, Mattson CL, Goldberger BA, Gladden RM (2017): Deaths involving fentanyl, fentanyl analogs, and U-47700—10 states, July-December 2016. MMWR Morb Mortal Wkly Rep 66:1197–1202.
2. Rudd RA, Seth P, David F, Scholl L (2016): Increases in drug and opioid-involved overdose deaths—United States, 2010-2015. MMWR Morb Mortal Wkly Rep 65:1445–1452.
3. Becker JAJ, Kieffer BL, Le Merrer J (2017): Differential behavioral and molecular alterations upon protracted abstinence from cocaine versus morphine, nicotine, THC and alcohol. Addict Biol 22:1205–1217.
4. Befort K, Filliol D, Ghate A, Darcq E, Matifas A, Muller J, *et al.* (2008): Mu-opioid receptor activation induces transcriptional plasticity in the central extended amygdala. Eur J Neurosci 27:2973–2984.
5. Le Merrer J, Befort K, Gardon O, Filliol D, Darcq E, Dembele D, *et al.* (2012): Protracted abstinence from distinct drugs of abuse shows regulation of a common gene network. Addict Biol 17:1–12.
6. Bailly J, Del Rossi N, Runtz L, Li JJ, Park D, Scherrer G, *et al.* (2020): Targeting morphine-responsive neurons: Generation of a knock-in

mouse line expressing Cre recombinase from the Mu-opioid receptor gene locus. eNeuro 7:ENEURO.0433-19.2020.
7. Bachtell RK, Jones JD, Heinzerling KG, Beardsley PM, Comer SD (2017): Glial and neuroinflammatory targets for treating substance use disorders. Drug Alcohol Depend 180:156–170.
8. Lacagnina MJ, Rivera PD, Bilbo SD (2017): Glial and neuroimmune mechanisms as critical modulators of drug use and abuse. Neuropsychopharmacology 42:156–177.
9. Linker KE, Cross SJ, Leslie FM (2019): Glial mechanisms underlying substance use disorders. Eur J Neurosci 50:2574–2589.
10. Salter MW, Stevens B (2017): Microglia emerge as central players in brain disease. Nat Med 23:1018–1027.
11. Bidlack JM (2000): Detection and function of opioid receptors on cells from the immune system. Clin Diagn Lab Immunol 7:719–723.
12. Zou S, Fitting S, Hahn YK, Welch SP, El-Hage N, Hauser KF, *et al.* (2011): Morphine potentiates neurodegenerative effects of HIV-1 Tat through actions at mu-opioid receptor-expressing glia. Brain 134:3616–3631.
13. Maduna T, Audouard E, Dembele D, Mouzaoui N, Reiss D, Massotte D, *et al.* (2018): Microglia express Mu opioid receptor: Insights from transcriptomics and fluorescent reporter mice. Front Psychiatry 9:726.
14. Leduc-Pessah H, Weilinger NL, Fan CY, Burma NE, Thompson RJ, Trang T (2017): Site-specific regulation of P2X7 receptor function in microglia gates morphine analgesic tolerance. J Neurosci 37:10154–10172.
15. Badimon A, Strasburger HJ, Ayata P, Chen X, Nair A, Ikegami A, *et al.* (2020): Negative feedback control of neuronal activity by microglia. Nature 586:417–423.
16. Merlini M, Rafalski VA, Ma K, Kim KY, Bushong EA, Rios Coronado PE, *et al.* (2021): Microglial Gi-dependent dynamics regulate brain network hyperexcitability. Nat Neurosci 24:19–23.
17. Campbell LA, Avdoshina V, Rozzi S, Mocchetti I (2013): CCL5 and cytokine expression in the rat brain: Differential modulation by chronic morphine and morphine withdrawal. Brain Behav Immun 34:130–140.
18. Hutchinson MR, Lewis SS, Coats BD, Skyba DA, Crysdale NY, Berkelhammer DL, *et al.* (2009): Reduction of opioid withdrawal and potentiation of acute opioid analgesia by systemic AV411 (ibudilast). Brain Behav Immun 23:240–250.
19. Burma NE, Bonin RP, Leduc-Pessah H, Baimel C, Cairncross ZF, Mousseau M, *et al.* (2017): Blocking microglial pannexin-1 channels alleviates morphine withdrawal in rodents. Nat Med 23:355–360.
20. Cai Y, Kong H, Pan YB, Jiang L, Pan XX, Hu L, *et al.* (2016): Procyanidins alleviates morphine tolerance by inhibiting activation of NLRP3 inflammasome in microglia. J Neuroinflammation 13:53.
21. Gessi S, Borea PA, Bencivenni S, Fazzi D, Varani K, Merighi S (2016): The activation of mu-opioid receptor potentiates LPS-induced NF-kB promoting an inflammatory phenotype in microglia. FEBS Lett 590:2813–2826.
22. Grace PM, Strand KA, Galer EL, Urban DJ, Wang X, Baratta MV, *et al.* (2016): Morphine paradoxically prolongs neuropathic pain in rats by amplifying spinal NLRP3 inflammasome activation. Proc Natl Acad Sci U S A 113:E3441–E3450.
23. Jacobsen JH, Watkins LR, Hutchinson MR (2014): Discovery of a novel site of opioid action at the innate immune pattern-recognition receptor TLR4 and its role in addiction. Int Rev Neurobiol 118:129–163.
24. Zhang Y, Li H, Li Y, Sun X, Zhu M, Hanley G, *et al.* (2011): Essential role of toll-like receptor 2 in morphine-induced microglia activation in mice. Neurosci Lett 489:43–47.
25. Sakers K, Lake AM, Khazanchi R, Ouwenga R, Vasek MJ, Dani A, *et al.* (2017): Astrocytes locally translate transcripts in their peripheral processes. Proc Natl Acad Sci U S A 114:E3830–E3838.
26. Haimon Z, Volaski A, Orthgiess J, Boura-Halfon S, Varol D, Shemer A, *et al.* (2018): Re-evaluating microglia expression profiles using RiboTag and cell isolation strategies. Nat Immunol 19:636–644.
27. Contet C, Filliol D, Matifas A, Kieffer BL (2008): Morphine-induced analgesic tolerance, locomotor sensitization and physical dependence do not require modification of mu opioid receptor, cdk5 and adenylate cyclase activity. Neuropharmacology 54:475–486.
28. Corder G, Tawfik VL, Wang D, Sypek EI, Low SA, Dickinson JR, *et al.* (2017): Loss of mu opioid receptor signaling in nociceptors, but not microglia, abrogates morphine tolerance without disrupting analgesia. Nat Med 23:164–173.
29. Lesiak AJ, Coffey K, Cohen JH, Liang KJ, Chavkin C, Neumaier JF (2021): Sequencing the serotonergic neuron translatome reveals a new role for Fkbp5 in stress. Mol Psychiatry 26:4742–4753.
30. Afgan E, Baker D, van den Beek M, Blankenberg D, Bouvier D, Cech M, *et al.* (2016): The Galaxy platform for accessible, reproducible and collaborative biomedical analyses: 2016 update. Nucleic Acids Res 44:W3–W10.
31. Patro R, Duggal G, Love MI, Irizarry RA, Kingsford C (2017): Salmon provides fast and bias-aware quantification of transcript expression. Nat Methods 14:417–419.
32. Levinstein MR, Coffey KR, Marx RG, Lesiak AJ, Neumaier JF (2020): Stress induces divergent gene expression among lateral habenula efferent pathways. Neurobiol Stress 13:100268.
33. Love MI, Huber W, Anders S (2014): Moderated estimation of fold change and dispersion for RNA-seq data with DESeq2. Genome Biol 15:550.
34. Liao Y, Wang J, Jaehnig EJ, Shi Z, Zhang B (2019): WebGestalt 2019: Gene set analysis toolkit with revamped UIs and APIs. Nucleic Acids Res 47:W199–W205.
35. Langfelder P, Horvath S (2008): WGCNA: An R package for weighted correlation network analysis. BMC Bioinformatics 9:559.
36. R Development Core Team (2010): R: A Language and Environment for Statistical Computing. Vienna, Austria: R Foundation for Statistical Computing.
37. Cobeldick S (2021): Convert Between RGB and Color Names. MATLAB Central File Exchange. Available at: https://www.mathworks.com/matlabcentral/fileexchange/48155-convert-between-rgb-and-color-names. Accessed July 9, 2019.
38. York EM, LeDue JM, Bernier LP, MacVicar BA (2018): 3DMorph automatic analysis of microglial morphology in three dimensions from ex vivo and in vivo imaging. eNeuro 5:ENEURO.0266-18.2018.
39. McKenzie AT, Wang M, Hauberg ME, Fullard JF, Kozlenkov A, Keenan A, *et al.* (2018): Brain cell type specific gene expression and co-expression network architectures. Sci Rep 8:8868.
40. Langfelder P, Zhang B, Horvath S (2008): Defining clusters from a hierarchical cluster tree: the Dynamic Tree Cut package for R. Bioinformatics 24:719–720.
41. Bernier LP, Bohlen CJ, York EM, Choi HB, Kamyabi A, Dissing-Olesen L, *et al.* (2019): Nanoscale surveillance of the brain by microglia via cAMP-regulated filopodia. Cell Rep 27:2895–2908.e2894.
42. Gerrits E, Heng Y, Boddeke E, Eggen BJL (2020): Transcriptional profiling of microglia; current state of the art and future perspectives. Glia 68:740–755.
43. Allen PB, Greenfield AT, Svenningsson P, Haspeslagh DC, Greengard P (2004): Phactrs 1-4: A family of protein phosphatase 1 and actin regulatory proteins. Proc Natl Acad Sci U S A 101:7187–7192.
44. Han H, Dong Z, Jia Y, Mao R, Zhou Q, Yang Y, *et al.* (2015): Opioid addiction and withdrawal differentially drive long-term depression of inhibitory synaptic transmission in the hippocampus. Sci Rep 5:9666.
45. Quina LA, Tempest L, Ng L, Harris JA, Ferguson S, Jhou TC, *et al.* (2015): Efferent pathways of the mouse lateral habenula. J Comp Neurol 523:32–60.
46. Jing F, Zhang Y, Long T, He W, Qin G, Zhang D, *et al.* (2019): P2Y12 receptor mediates microglial activation via RhoA/ROCK pathway in the trigeminal nucleus caudalis in a mouse model of chronic migraine. J Neuroinflammation 16:217.
47. Gu N, Eyo UB, Murugan M, Peng J, Matta S, Dong H, *et al.* (2016): Microglial P2Y12 receptors regulate microglial activation and surveillance during neuropathic pain. Brain Behav Immun 55:82–92.
48. Horvath G, Goloncser F, Csolle C, Kiraly K, Ando RD, Baranyi M, *et al.* (2014): Central P2Y12 receptor blockade alleviates inflammatory and neuropathic pain and cytokine production in rodents. Neurobiol Dis 70:162–178.